JBC RESEARCH ARTICLE

The toxin mimic FS48 from the salivary gland of *Xenopsylla cheopis* functions as a Kv1.3 channel-blocking immunomodulator of T cell activation

Received for publication, May 17, 2021, and in revised form, November 14, 2021 Published, Papers in Press, December 14, 2021,
https://doi.org/10.1016/j.jbc.2021.101497

Qingye Zeng[1,‡], Wancheng Lu[1,‡], Zhenhui Deng[1], Bei Zhang[1], Jiena Wu[1], Jinwei Chai[1], Xin Chen[2], and Xueqing Xu[1,*]

From the [1]Guangdong Provincial Key Laboratory of New Drug Screening, School of Pharmaceutical Sciences, and [2]Department of Pulmonary and Critical Care Medicine, Zhujiang Hospital, Southern Medical University, Guangzhou, China

Edited by Mike Shipston

The Kv1.3 channel has been widely demonstrated to play crucial roles in the activation and proliferation of T cells, which suggests that selective blockers could serve as potential therapeutics for autoimmune diseases mediated by T cells. We previously described that the toxin mimic FS48 from salivary gland of *Xenopsylla cheopis* downregulates the secretion of proinflammatory factors by Raw 264.7 cells by blocking the Kv1.3 channel and the subsequent inactivation of the proinflammatory MAPK/NF-κB pathways. However, the effects of FS48 on human T cells and autoimmune diseases are unclear. Here, we described its immunomodulatory effects on human T cells derived from suppression of Kv1.3 channel. Kv1.3 currents in Jurkat T cells were recorded by whole-cell patch-clamp, and Ca^{2+} influx, cell proliferation, and TNF-α and IL-2 secretion were measured using Fluo-4, CCK-8, and ELISA assays, respectively. The *in vivo* immunosuppressive activity of FS48 was evaluated with a rat DTH model. We found that FS48 reduced Kv1.3 currents in Jurkat T cells in a concentration-dependent manner with an IC_{50} value of about 1.42 μM. FS48 also significantly suppressed Kv1.3 protein expression, Ca^{2+} influx, MAPK/NF-κB/NFATc1 pathway activation, and TNF-α and IL-2 production in activated Jurkat T cells. Finally, we show that FS48 relieved the DTH response in rats. We therefore conclude that FS48 can block the Kv1.3 channel and inhibit human T cell activation, which most likely contributes to its immunomodulatory actions and highlights the great potential of this evolutionary-guided peptide as a drug template in future studies.

Kv1.3 channel belongs to the Shaker group of potassium channels, which is highly expressed in effector memory T (T_{EM}) cells and makes up the dominant K^+ conductance for these cells (1). Kv1.3 channel in company with K_{Ca} channel (Ca^{2+} activated-potassium) mediates the cell resting membrane potential and provides the electrochemical driving force for Ca^{2+} influx through the CRAC (Ca^{2+} release-activated Ca^{2+}) channel. Increased intracellular Ca^{2+} activated the nuclear factor of activate T cells c1 (NFATc1) and nuclear factor NF-κB, which mediate the activation, proliferation, and the secretion of cytokines of T cells, such as TNF-α and IL-2 (2, 3). Many studies have proved that blockage of Kv1.3 channel causes the inhibition of Ca^{2+} influx and the production of proinflammatory cytokines, thus exhibiting anti-inflammatory and immunomodulatory effects (4–9). In many autoimmune animal models such as delayed-type hypersensitivity (DTH), type I diabetes, rheumatoid arthritis, chronic asthma, multiple sclerosis, psoriasis and diseases associated T_{EM} cells are reported to remarkably increase Kv1.3 channel expression, migrate into tissues, release inflammatory cytokines, and cause detrimental inflammatory reaction after activation (8–10). The proliferation and cytokine secretion of these cells can be suppressed by Kv1.3 inhibitors (1, 10–14). Consequently, Kv1.3 has been regarded as a novel therapeutic target for many T-cell-mediated autoimmune diseases (8, 10). Hence, the discovery and development of specific Kv1.3 inhibitors have been widely carried out to prepare novel immunomodulators and immunosuppressants.

Natural peptide toxins are gradually acknowledged as potential therapeutic option for many diseases, which is attributed to their antitumor, immunomodulation, analgesic, and antimicrobial properties (8, 15). We previously identified and characterized FS48, a novel potassium channel inhibitor from the salivary gland of *Xenopsylla cheopis* (16). FS48 downregulates the secretion of proinflammatory NO, IL-1β, IL-6, and TNF-α by Raw 264.7 cells *via* Kv1.3 channel blockage and expression suppression as well as MAPK/NF-κB pathway inactivation. The present study aimed to evaluate the blocking effect of FS48 on Kv1.3 channel in human T cells and to clear its immunomodulatory mechanism. We first determined the effect of FS48 on the Kv1.3 channels and Ca^{2+} influx as well as its downstream signaling pathways. Moreover, we examined the effect of FS48 on the production of TNF-α and IL-2 with Kv1.3-siRNA. Finally, a DTH model was used to identify the immunomodulatory effect of FS48 *in vivo*. Our results show for the first time that FS48 inhibits Kv1.3-mediated currents, decreases Ca^{2+} influx and Ca^{2+}-activated transcriptional factors, correspondingly suppressing the activation, proliferation,

‡ These authors contributed equally to this work.
* For correspondence: Xueqing Xu, xu2003@smu.edu.cn.

the release of IL-2 and TNF-α of Jurkat T cells. Therefore, we may conclude that FS48 can act in T cells and play an immunomodulatory role through Kv1.3 channel.

Results

FS48 blocked Kv1.3 channel currents in Jurkat T cells

We performed patch-clamp electrophysiological recording assay in the whole-cell mode to evaluate the effect of FS48 on Kv1.3 currents in Jurkat T cells. As shown in Figure 1*A*, at test potentials positive to +40 mV, the blocking effects of FS48 at the concentrations from 0.1 to 10 μM on Kv1.3 channels were demonstrated to be concentration-dependent and the highest concentration of FS48 decreased the Kv1.3 currents by 75.42% ± 7.48% (n = 5) (Fig. 1*A*). Meanwhile, 100 nM MgTx significantly reduced the current by 93.75% ± 3.58% (n = 5). The Hill equation analysis showed the IC_{50} value of FS48 on Kv1.3 peak current was calculated to be 1.42 ± 0.12 μM (Fig. 1*B*). Moreover, the current–voltage curve indicated that FS48 didn't affect the property and the activation of Kv1.3 channels (Fig. 1*C*), which was the same as our previous observed in cloned human Kv1.3 channels of HEK-293T and Raw 264.7 cells.

FS48 inhibited Kv1.3 protein expression

Cell viability measurements showed that FS48 at the concentrations from 0 to 30 μM for up to 24 h didn't inhibit or promote Jurkat T cells survival (Fig. 2*A*). In order to identify whether FS48 can inhibit Kv1.3 protein expression, Jurkat T cells were incubated with FS48 and MgTx for 8 h and 24 h before quantitative real-time PCR (qRT-PCR) and Western blot analysis, respectively. As shown in Figure 2, *B–D*, 3 μM FS48 did not modify Kv1.3 mRNA but reduced the amount of Kv1.3 channel protein by 24.67% ± 5.64%. However, 24 h pretreatment with MgTX (50, 100, and 200 nM) had no obvious effects on Kv1.3 channel protein expression ($p > 0.05$) (Figs. 2, *C* and *D* and S2).

FS48 suppressed the Ca^{2+} influx to Ca^{2+}-depleted Jurkat T cells

It has been proved that Kv1.3 channels play a critical role in the Ca^{2+} homeostasis of T cells by keeping the resting membrane potential, and the inhibition of Kv1.3 channel markedly decreases the Ca^{2+} influx (2, 3). To test this hypothesis, we used Fluo4-AM, a fluorescent probe widely used in measuring the content of intracellular Ca^{2+} to identify the effect of FS48 on changes of intracellular Ca^{2+} concentrations. Compared with the negative control, PMA/ionomycin induced a significant release of Ca^{2+} from the endoplasmic reticulum and rise in the cytoplasm of Jurkat T cells. However, when cells were treated by 3 μM FS48 and 100 nM MgTx, the increasing concentration of Ca^{2+} was reduced, which was indicated by the left shift of fluorescence signal compared with PMA/ionomycin-treated group (Fig. 3*A*). To further explore whether FS48 inhibited Ca^{2+} change of the cells, we measure Ca^{2+} concentration in response to TG and $CaCl_2$ stimulation. As shown in Figure 3, *B–D* and Fig. S3, in Ca^{2+}-free Ringer's solution, treatment with 1 μM TG rose slightly the intracellular Ca^{2+} concentration. Incubation with 0.1 and 1 μM FS48 as well as 1 nM MgTx did not change the Ca^{2+} release induced by TG ($p > 0.05$), while 10 μM FS48 and MgTx at the concentration of 10 nM and 100 nM significantly inhibited this Ca^{2+} influx response (Figs. 3*C* and S3*B*). However, it was obviously observed that the readdition of Ca^{2+} to Ca^{2+}-depleted cells induced significant intracellular Ca^{2+} increase after cell treatment with TG followed by addition of 2 mM $CaCl_2$, which was concentration-dependently blunted by FS48 and MgTx at three tested concentrations by 25.36% ± 6.54%, 39.29% ± 4.39%, 64.29% ± 8.45% and 24.28% ± 2.15%, 49.46% ± 2.23%, and 53.51% ± 1.68% of the maximum Ca^{2+} influx, respectively (Figs. 3*D* and S3*C*). Taken together, these results demonstrate that FS48 like MgTx is a strong suppressor of intracellular Ca^{2+} signaling of T cells *via* blockage of Kv1.3 channel.

FS48 downregulated the Ca^{2+}-related transcription factors

Ca^{2+} influx as well as Ca^{2+}-related signal pathway factors, such as NF-κB, NFATc1 and MAPK (ERK, JNK and p38), mediate the activation of human T cells (2). To further explore the mechanism through which FS48 inhibited T cell activation, Western blot analysis was performed to investigate the effects of FS48 on the activation of NF-κB, NFATc1 and MAPK signaling pathways induced by PMA/ionomycin. Figure 4

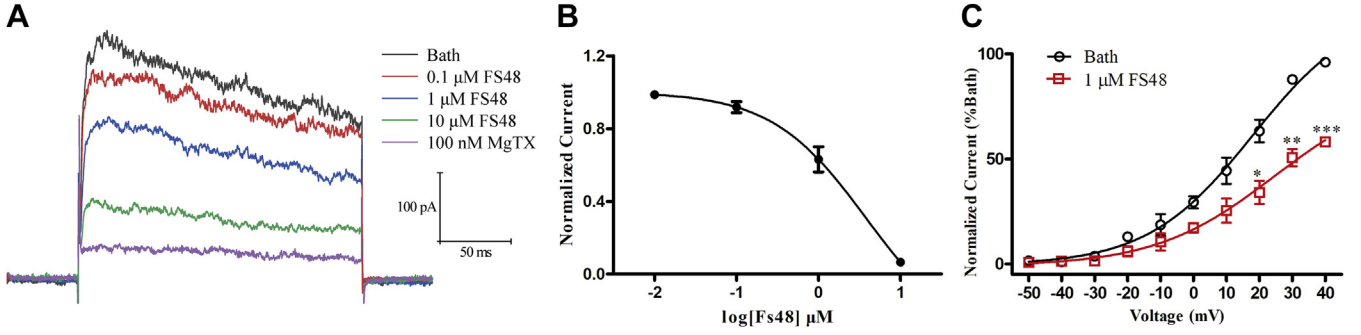

Figure 1. Modulation of FS48 on endogenous voltage-gated potassium channels. *A*, representative traces of MgTx and different concentrations of FS48 suppressing the Kv1.3 currents in Jurkat T cells. Currents were elicited by applying 200 ms depolarization pulses from a holding potential of −70 mV to +40 mV in Jurkat T cells. *B*, concentration–response curve of FS48 inhibiting Kv1.3 currents in Jurkat T cells. Currents were normalized to the control and fitted by a Hill equation. *C*, current–voltage relationships (I-V). Test potentials were ranged from −50 mV to +40 mV with 10 mV increment steps. Y-axis represents the currents at different activation potential and normalized to the bath current at +40 mV in the present (*red*) or absent (*black*) of FS48; The *solid lines* represent the average Boltzmann sigmoidal fits. Data are shown as mean ± SD (n ≥ 3). *$p < 0.05$, **$p < 0.01$, ***$p < 0.001$ compared with bath group.

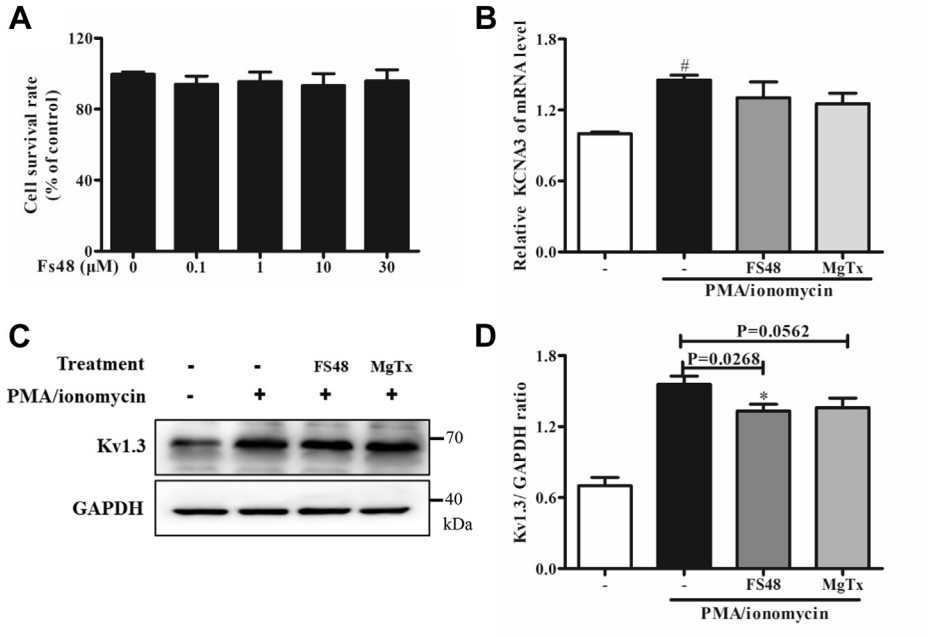

Figure 2. Effects of FS48 on mRNA and protein expression of Kv1.3 channel. *A*, the viability of Jurkat T cells incubated with indicated concentrations of FS48 for 24 h. *B*, the relative expression analysis of KCNA3 mRNA in the presence and absence of FS48 and MgTx by qRT-PCR. *C*, Kv1.3 protein expression analysis of Kv1.3 channel. The cells were treated with PMA/ionomycin (50 ng/ml; 1 μg/ml) for 24 h after incubated with 3 μM FS48 and 100 nM MgTx for 1 h and then were collected for Western blot analysis. *D*, the ratios of Kv1.3 proteins to GAPDH. Quantity One software (Bio-Rad) was used for band density analysis. Data are shown as mean ± SD (n ≥ 3). $^{\#}p < 0.05$, compared with negative control group. $^{*}p < 0.05$, compared with model group.

showed that PMA/ionomycin treatment markedly increased nuclear translocation of NF-κB p65 and NFATc1 as well as the phosphorylation of ERK, JNK as well as p38. However, both 3 μM FS48 and 100 nM MgTx significantly moderated the phosphorylation of ERK, JNK, and p38 and the nuclear translocation of NF-κB p65 and NFATc1.

FS48 reduced cell proliferation and IL-2 as well as TNF-α production

In order to determine whether the inhibition of Kv1.3 channel and Ca^{2+} signaling pathways by FS48 might cause the immunoregulatory effect as was reported for Acacetin and Lovastatin (5, 6), we further investigated the effect of FS48 on

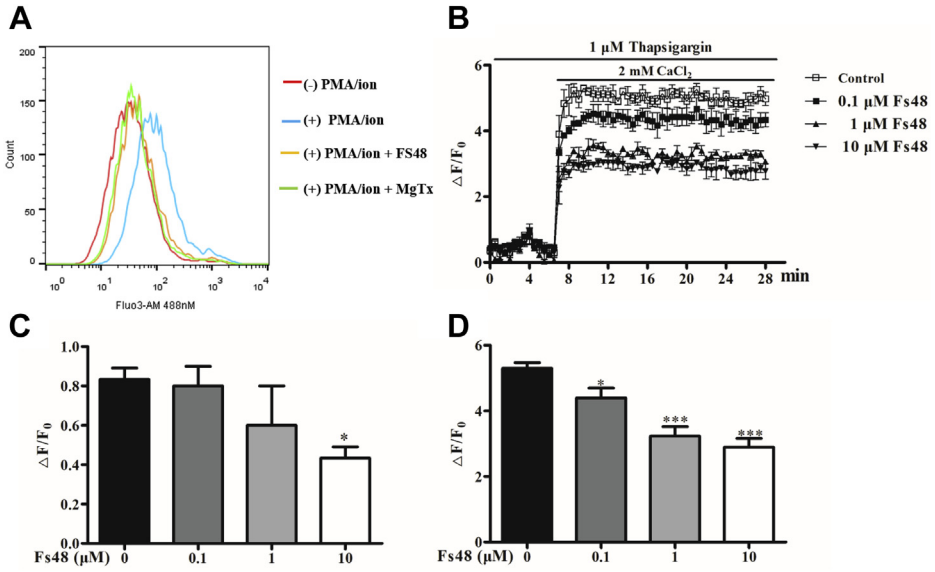

Figure 3. Effect of FS48 on the Ca^{2+} influx to Ca^{2+}-depleted Jurkat T cells. *A*, flow cytometry analysis of the concentration of intracellular Ca^{2+} in Jurkat T cells. *B*, the summarized time course of the suppressed Ca^{2+} influx to Ca^{2+}-depleted Jurkat T cells by FS48. Jurkat T cells were incubated with Fluo4-AM, resuspended in Ca^{2+} -free Ringer solution, and treated with 0, 0.1, 1, and 10 μM FS48 for 20 min before the intracellular Ca^{2+} release, and Ca^{2+} influx was elicited by TG and $CaCl_2$, respectively. The fluorescence signals were read using microplate spectrophotometer. *C*, the $\Delta F/F_0$ value of the peak intracellular Ca^{2+} release response stimulated by TG. *D*, the $\Delta F/F_0$ value of the maximum Ca^{2+} influx response after 2 mM $CaCl_2$ application. All data are presented as mean ± SD (n ≥ 3). $^{*}p < 0.05$, $^{***}p < 0.001$, compared with negative control group.

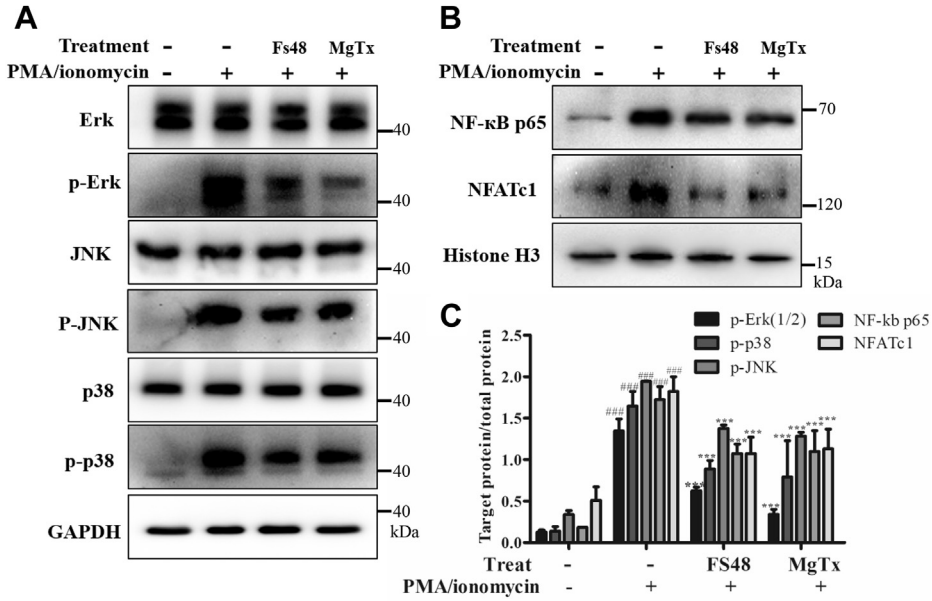

Figure 4. Effect of FS48 on the activation of MAPK/NF-κB/NFATc1 pathway. Jurkat T cells were pretreated with 3 μM FS48 and 100 nM MgTx for 1 h, then the cells were stimulated with PMA/ionomycin (50 ng/ml; 1 μg/ml) for 4 h before collected for Western blot analysis. *A* and *B*, representative Western blot analysis of NF-κB p65 and NFATc1 nuclear translocation, ERK, JNK, and p38 phosphorylation. *C*, the ratios of p65 and NFATc1 protein to Histone H3 and phosphorylated ERK, JNK, and p38 to corresponding total protein. Quantity One software (Bio-Rad) was used for band density analysis. All data are shown as mean ± SD (n ≥ 3). $^{###}p < 0.001$, compared with negative control group; $^{***}p < 0.001$ compared with model group.

the proliferation and expression of TNF-α and IL-2 from PMA/ionomycin-triggered Jurkat T cells. As illustrated in Figure 5, both FS48 and MgTx suppressed TNF-α and IL-2 mRNA expression stimulated by PMA/ionomycin. Moreover, both MgTx and FS48 also inhibited the cell proliferation and secretion of TNF-α and IL-2 protein in supernatant with a concentration-dependent manner. We found that treatment with 0.1, 1, 10 μM FS48, and 100 nM MgTx resulted in secretion inhibition of 20.74% ± 4.52%, 39.68% ± 10.50%, 69.04% ± 7.41%, 50.23% ± 7.32% TNF-α and 9.89% ± 6.49%, 21.75% ± 4.96%, 63.73% ± 11.49%, 55.78% ± 6.25% IL-2, respectively. Furthermore, in order to verify whether the inhibition of TNF-α and IL-2 secretion by FS48 was related to Kv1.3 channel, we suppressed Kv1.3 expressions with specific Kv1.3 siRNA in Jurkat T cells. We found that siRNA1 was the most effective siRNA and caused 56.67% ± 4.11% knockdown of Kv1.3 channel, while siRNA-NC caused no apparent change. Importantly, although FS48 and MgTx also decreased TNF-α and IL-2 secretion in Kv1.3 knockdown Jurkat T cells in concentration-dependent manner, their inhibitory effects

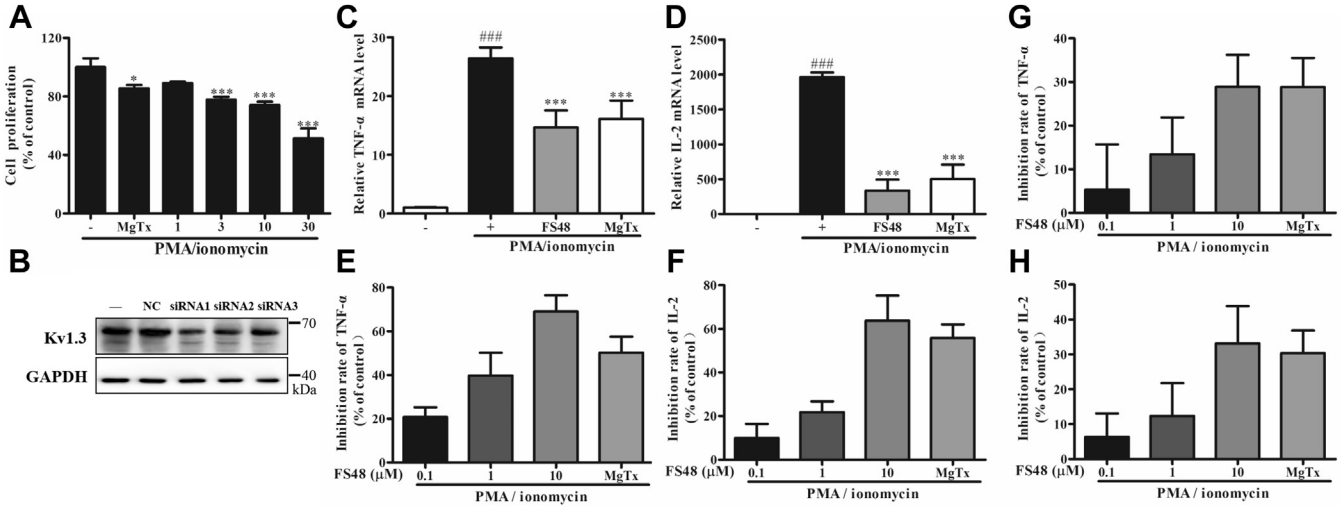

Figure 5. Effect of FS48 on the secretion of TNF-α and IL-2 in Jurkat T cells stimulated with PMA/ionomycin. *A*, effect of FS48 (1, 3, 10, 30 μM) and 100 nM MgTx on the proliferation of Jurkat T cells stimulated with PMA/ionomycin. *B*, knockdown of Kv1.3 channel expression with different siRNA. *C* and *D*, the mRNA production of TNF-α and IL-2. *E* and *F*, the inhibition rate of TNF-α and IL-2 secretion in Jurkat T cells. *G* and *H*, the inhibition rate of TNF-α and IL-2 in Jurkat T cells after knockdown Kv1.3. All data are presented as mean ± SD (n ≥ 3). $^{###}p < 0.001$, compared with negative control group; $^{*}p < 0.05$, $^{***}p < 0.001$ compared with model group.

were significantly reduced and the same concentration of FS48 and MgTx inhibited 5.31% ± 8.48%, 13.4% ± 6.92%, 28.9% ± 5.99%, 28.81% ± 5.47% TNF-α secretion and 6.34% ± 5.51%, 12.35% ± 7.69%, 33.15% ± 8.75%, 30.37% ± 5.30% IL-2 secretion after knockdown of Kv1.3 channel. These results indicated that FS48 exerts its immunosuppression effect most likely through Kv1.3 channels and may be a new lead drug template for autoimmune diseases.

FS48 attenuated DTH reactions in vivo

The DTH reaction in which the cell-mediated pathologic response involves T cell activation is a perfect model investigating the *in vivo* effects of Kv1.3 blockers (1, 13). Thus, we evaluated the immunosuppressive activity of FS48 in a rat model of DTH. When compared with the control ears, OVA induced a pronounced swelling caused by inflammatory reaction in the challenged ear. However, when treated with FS48 and MgTx, ear swelling induced by OVA was markedly ameliorated by 47.33% ± 5.32% (Figs. 6, *A* and *B* and S1). Consistent with the measurement results of ear thickness, TNF-α and IL-2 expressions in OVA-changed tissues were also increased in the model group (Fig. 6, *C* and *D*). In addition, histological sections of auricle tissue showed that the OVA-challenged ears of DTH rats suffered from edema and infiltration of leukocytes into the epidermis and dermis, which were significantly suppressed by FS48 (Fig. 6*E*). Together, these results suggest that FS48 could significantly suppress the OVA-induced DTH reaction probably through inhibiting lymphocyte function.

Discussion

Kv1.3 constitutes the main K^+ channel expressed in human T cells and plays a crucial role to maintain the resting membrane potential, which provides electrochemical driving force for Ca^{2+} influx. Blocking Kv1.3 channel can cause the depolarization of the membrane potential (17), decrease of Ca^{2+} influx, inhibition of the gene expression of IL-2 and TNF-α, and finally suppression of the proliferation and activation of T cells (1, 2, 7, 9, 18, 19). These characteristic features are clearly demonstrated by Kv1.3 peptide inhibitors from scorpions (CHTX, KTX, and MgTx) (1, 9, 17, 20, 21), and from sea anemones (ShK) (22). Similar with these Kv1.3 blockers (4, 8, 9, 23), FS48 at tested concentrations displays inhibitory effects on the depolarization of the membrane potential, Ca^{2+} influx, the Ca^{2+}-dependent activation of MAPK/NF-κB/NFATc1 signal, T cell proliferation, and production of IL-2 as well as TNF-α stimulated by PMA/ionomycin, which can be significantly attenuated by siRNA knockdown of Kv1.3 channels (1, 24). Furthermore, FS48 can also suppress Kv1.3 protein expression after 24 h incubation with activated Jurkat T cells (Fig. 2, *C* and *D*), which will extend the blocking effect of FS48 on Kv1.3 channels and damage the function of T-cell. Finally, FS48 ameliorates the DTH response in rats. To conclude, FS48 can decrease T-cell activation in T-cell-mediated pathological conditions by blocking the Kv1.3 currents and channel protein expression *in vivo*.

Zhi Li proposes that a calcium-dependent pathway might be involved in the transcription of KCNA3 gene (23). Thus, the upregulation of the Kv1.3 channel may be driven by Ca^{2+} influx and suppressed by channel inhibitors due to a cross talk between channel activity and channel expression in T cells. Consistently, our data (Fig. 2, *B–D*) have demonstrated a correlation between enhanced intracellular Ca^{2+} concentration and Kv1.3 expression in activated T cells (4, 23). Interestingly, it has been previously demonstrated that pretreatment with ADWX-1, Diclofenac, and 18β-GA for 24 h shows no significant effect on KCNA3 mRNA level in nonactivated T-cells but significantly reduces its increase in activated T cells with increased intracellular Ca^{2+} concentration (4, 23, 25). Consistent with the effects of these inhibitors in nonactivated T cells, our data in Fig. S4 demonstrate that neither FS48 nor MgTX regulates KCNA3 gene transcription in Jurkat T cells without PMA/ionomycin stimulation. Such an effect for MgTx has already been reported by Conforti (26). Our data also demonstrate that FS48 and MgTx can't lower the enhanced KCNA3 mRNA expression in Jurkat T cells stimulated by PMA/ionomycin. More specifically, both FS48 and MgTx at tested concentrations can't abolish the PMA/ionomycin-induced Ca^{2+} influx as judged from the flow cytometry analysis of the intracellular Ca^{2+} concentration in Jurkat T cells (Fig. 3*A*). As a result, residual Ca^{2+} increase consequently promotes upregulation of KCNA3 gene transcription, thus proving that FS48 and MgTx can't decrease the increasing KCNA3 mRNA expression in Jurkat T cells stimulated by PMA/ionomycin. Remarkably, Villalonga *et al.* (25) have reported that PHA/PMA can't change the mRNA and protein levels of Kv1.3 in Jurkat T cells, and it is known that Sp1 transcription factor regulates Kv1.3 expression by directly binding to the promoter region of KCNA3 gene in the nucleus of A549 cells (27). Therefore, other complex regulation mechanisms unrelated to Ca^{2+} concentration maybe be also responsible for the transcription regulation of KCNA3 gene. It has also been previously demonstrated that the expression regulation of Kv1.3 protein takes place at a posttranscriptional level, independent of changes in mRNA expression (5, 7, 26, 28). As a result, the decreased expression of Kv1.3 channels in activated T cells is not in agreement with its mRNA levels. In this study, our data suggest that downregulation of Kv1.3 channel expression by FS48 treatment occurs posttranscriptionally, similar to the effects reported for hypoxia, DPO-1 and Acacetin, which can also lower Kv1.3 expression in the protein level with unchangeable mRNA expression (5, 7, 26). It is known that (a) pretreatment of Jurkat T cells with DPO-1 for 24 h rather than 30 min significantly reduces the Kv1.3 channel protein expression but (b) 30 min incubation with DPO-1 also inhibits the Ca^{2+} influx in Ca^{2+}-depleted Jurkat T cells (7), thus suggesting a different mechanism of action between DPO-1 and FS48. Phosphorylation mechanisms can affect protein synthesis at the initiation or elongation phase (29). To conclude, changes in channel protein synthesis,

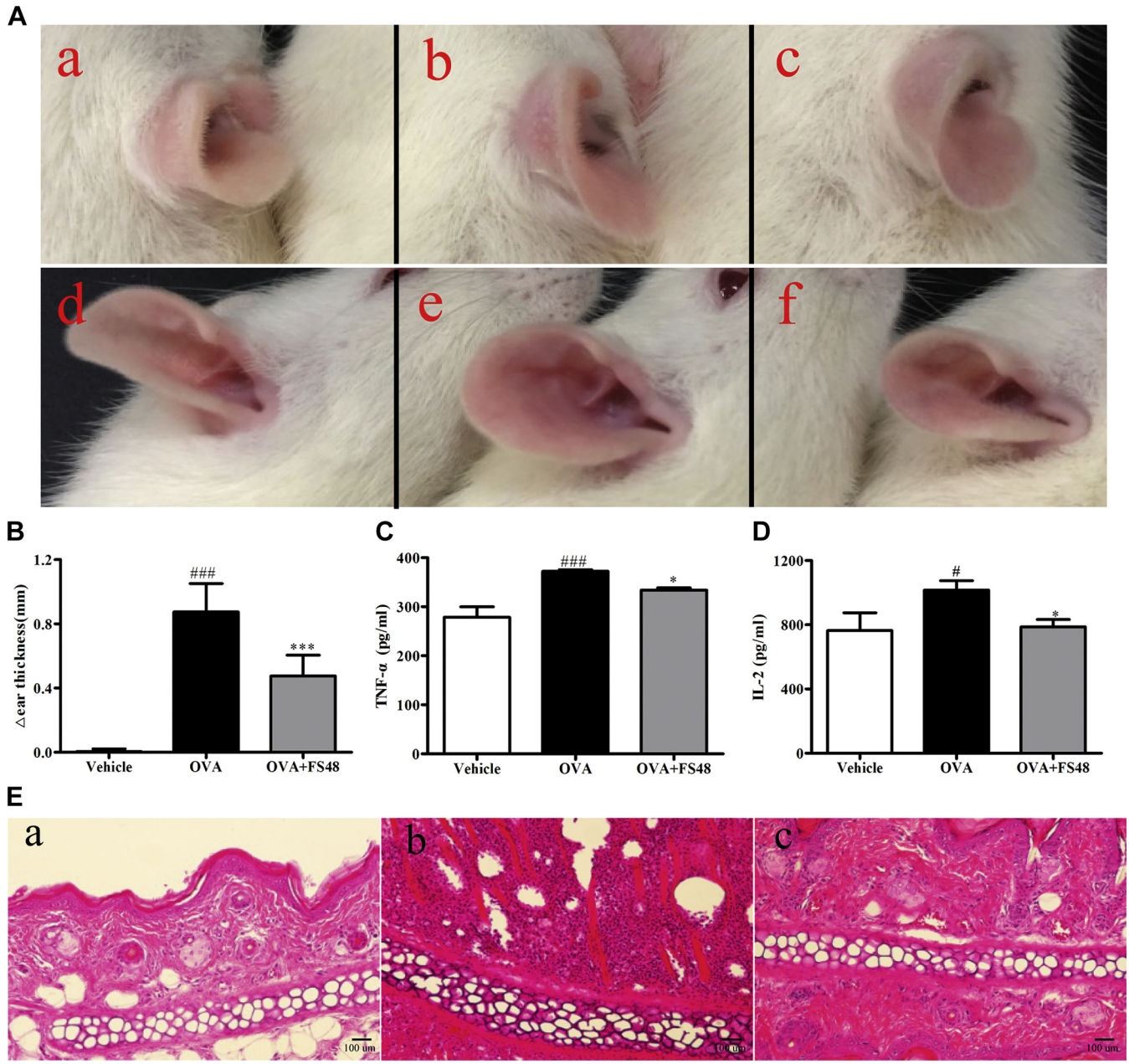

Figure 6. DTH immunosuppressive effects of FS48. *A*, photographic images of rat ear edemas. Photographs at 24 h postinjection show the gross pathology of ear from saline (a and d), OVA plus saline (b and e), OVA plus 2.5 mg/kg FS48 (c and f) groups. The top and lateral views of ears are displayed in parts a–c and d–f, respectively. *B*, the thickness increase between the OVA-challenged ear and the saline-treated ear in each group (n = 6) 24 h after the second challenge. *C* and *D*, the summarized secretion of TNF-α and IL-2 in the ear tissue. *E*, histology analysis of rat auricle tissue sections in vehicle (Panel a), OVA-treated (Panel b) and OVA +2.5 mg/kg FS48-treated DTH rats (Panel c) in 24 h (Original magnification, ×100). Data were showed as means ± SD, $^{###}p < 0.001$ compared with vehicle group; $^{*}p < 0.05$ and $^{***}p < 0.001$ compared with model group.

degradation, or other posttranscriptional modification are likely responsible for the observed decreased Kv1.3 expression in PMA/ionomycin-stimulated Jurkat T cells after FS48 treatment for 24 h. MgTx, like Lovastatin, does not change the expression of Kv1.3 channels in nonstimulated Jurkat T cells at both the mRNA and protein levels (Fig. S4) (6, 7, 26), but the specific peptide also shows similar lack of effects in the stimulated Jurkat T cells (Figs. 2, *C* and *D* and S2), a finding that makes the mechanism of MgTx action different from that induced by FS48 in the stimulated Jurkat T cells. Therefore, our data suggest a different posttranscriptional modification and regulation of the Kv1.3 expression in the presence of FS48 (when compared with MgTx), and further research is necessary to investigate the molecular mechanism, which mediates the observed difference in the action of MgTx and FS48.

It is reported that Kv1.3 channel expression is closely associated with the MAPK/NF-κB/NFATc1 signaling activation (30–35). Here, the activation of MAPK/NF-κB/NFATc1 pathways in Jurkat T cells stimulated by PMA/ionomycin can

be significantly suppressed by FS48 (Fig. 4), which is in line with its effects on macrophages and the effects of other Kv1.3 blockers on T_{EM} cells (30–35). Three activated kinases of MAPK pathway result in a cascade of downstream transcription factors that, in turn, cause T cell proliferation and the expression activation of Kv1.3. The suppression function of FS48 on signal cascade may partly explain the observed inhibition of Jurkat T cell proliferation and the Kv1.3 expression stimulated by PMA/ionomycin. The activation of MAPK pathway is necessary during DTH (36, 37), which directly or indirectly mediates the production of inflammatory cytokines such as TNF-α *in vivo* (38–40). The Kv1.3 blocking peptides such as MgTx, KTX, ShK-186, and BmKTX-D33H ameliorate autoimmune DTH reaction characterized by tissue swelling and infiltration in the subcutaneous layer and have no obvious side effects *in vivo* (9, 13, 22, 41–43). Consistent with these findings and its effects in Jurkat T cells, like MgTx, FS48 markedly suppresses the ear swelling (Figs. 6, *A* and *B* and S1), the production of TNF-α and IL-2 and inflammatory infiltrate in an OVA-induced DTH response (Fig. 6, *C–E*). These results further demonstrate that the immunoregulatory properties of FS48 on MAPK signal cascades. Furtherly, considering that FS48 displays anti-inflammatory effect *in vivo via* Kv1.3 channel blockage and expression suppression as well as MAPK/NF-κB pathway inactivation of macrophage, which is one important cellular component of DTH (16, 44, 45), we can speculate that the effects of FS48 on DTH should be due to its combined effects on two or more kinds of cells expressing Kv1.3 channels on their membranes. Notably, despite the fact that FS48 is a weak blocker of Kv1.3 channel when compared with the above toxin peptides which are known of displaying DTH suppression effects *in vitro*, it shows anti-inflammatory and immunomodulatory effects *in vivo*, which are relatively stronger in comparison with MgTx, KTX, ShK-186, and BmKTX-D33H (8, 9, 13, 22, 41–43). Two reasons may be responsible for this phenomenon. Firstly, given the lack effects of MgTx on the Kv1.3 expression, the channel expression inhibition mediated by FS48 in immune cells such as T-cells may strengthen its immunosuppression potential *in vivo*. Secondly, the higher immunogenicity or/and lower stability of MgTx when compared with FS48 might reduce the therapeutic efficacy *in vivo*. As shown by Fig. S5 and Tables S1–S3, which are derived from our bioinformatics-based prediction of B cell and T cell epitopes, MgTx has greater immunogenicity than FS48. Furthermore, the plasma half-life time of FS48 was about 353.1 min (Fig. S6), which is longer than the 120 min observed for MgTx by Koo *et al.* (42). Therefore, FS48 maybe be more stable than MgTx *in vivo*. However, further research with experimental animals treated by flea FS48 and MgTx is necessary to ensure the exact mechanism responsible for this phenomenon. Anyway, this still proves a therapeutic potential of FS48 as an ideal candidate molecule against human T-cell-mediated inflammatory diseases such as DTH, rheumatoid arthritis, and psoriasis, which can be reversed by Kv1.3 blockers *in vivo* (10, 46).

Taken together, our data suggest that FS48 exhibits an immunosuppressive effect *in vitro* and *in vivo*, probably by inhibiting proliferation and activation of lymphocytes *via* blocking Kv1.3 channels. This is the first report that a protein from the salivary gland of haematophagous arthropods can be involved in immunomodulation of T-cell-mediated immune response, which contributes to explain the blood-sucking mechanism of *X. cheopis*.

Experimental procedures

Materials and chemicals

RPMI-1640, fetal bovine serum, phosphate buffer saline (PBS), and penicillin/streptomycin were all from Gibco. Phorbol ester (PMA)/ionomycin, thapsigargin (TG), and fluo-4 AM were purchased from Sigma-Aldrich, Alomone Laboratories, and Invitrogen, respectively. All liquid stock was kept light protected in −20 °C. The human Jurkat T cell line was purchased from the China Center for Type Culture Collection, cultured with complete RPMI-1640 contained 10% FBS and 1% streptomycin/penicillin, and maintained at 37 °C under 5% CO_2 atmosphere. MgTx and primary antibodies against Kv1.3 were from Alomone Labs, p38, p-p38, ERK, p-ERK, JNK, p-JNK, Histone H3, NF-κB p65, NFATc1, GAPDH, and horseradish peroxidase–conjugated secondary antibodies were from Cell Signaling Technologies.

Electric recordings and analysis

Jurkat T cells were applied for the patch-clamp electrophysiological recordings in the whole-cell mode at 22 °C as previously described by us (47). The external solution was as follows (in mM): 5.9 KCl, 2.2 $CaCl_2$, 137 NaCl, 1.2 $MgCl_2$, 10 HEPES, and 14 D-glucose (adjusted to pH 7.3 with KOH) and the pipette solution contained (in mM): 140 KF, 2 Na_2ATP, 4 $MgCl_2$, 1 EGTA, and 10 HEPES (adjusted to pH 7.3 with KOH). Kv1.3 currents were evoked by a 200-ms depolarization to +40 mV from a holding potential of −80 mV. The pCLAMP 10.3 software and Igor pro were used to obtain and analyze data, respectively. The Hill equation for IC_{50} calculation as follows: $Y = 100/(1 + 10\text{-}((LogIC_{50} - X) \times H))$ (where y is the normalized response, X is the log of concentration, and H is the slope factor or Hill slope). For I/V curve measurements, recordings were performed with the activation potential to be from −50 mV to +40 mV with 10 mV increment steps. The data points in current–voltage relationships were fitted to the Boltzmann equation: $I/I_{max} = 1/[1 + \exp(V - V_{1/2})/k]$, where k is the slope factor and $V_{1/2}$ is the voltage for half-maximum activation.

Cell viability measurement

Cell viability and proliferation were measured with cell counting kit-8 (CCK-8) method. For cell survival assay, 5×10^4/well Jurkat T cells were seed into a 96-well plate and incubated with FS48 (0.1, 1, 10, 30 μM) for 24 h. For cell proliferation assay, 5×10^4/well Jurkat T cells were seed into a 96-well plate and incubated with FS48 (0.1, 1, 10, 30 μM) or 100 nM MgTx for 30 min before incubation with PMA/

ionomycin (50 ng/ml;1 μg/ml) for 24 h, the cells treated with PBS were used as a negative control. CCK-8 solution (10 μl) was applied into the wells for 3 h, and the absorbance value was read at 450 nm wavelength with a Microplate Reader (Tecan Company). The negative control group was calculated as 100% survival rate.

Quantitative real-time PCR

Jurkat T cells were seed into a 6-well plate and pretreated with 3 μM FS48 or 100 nM MgTx, a Kv1.3 channel blocker, for 1 h before incubation with PMA/ionomycin (50 ng/ml;1 μg/ml) for 8 h. The cells treated with PBS were used as a negative control. The total RNA of each group was extracted with Trizol and was used for the synthesis of cDNA with the reverse transcriptase (TaKaRa Biotechnology). Real-time PCR was carried out with Hieff qPCR SYBR Green Master Mix (Yeasen) in Light Cycler 480 system. In all experiments, a total of 40 amplification cycles was performed as previously reported (16). The primers sequences were listed in Table 1. The relative expression was quantified with $2^{-\Delta\Delta CT}$ method and normalized to the fold change of GAPDH mRNA. Each treatment was repeated at least three times.

Inflammatory cytokine measurement

Jurkat T cells were treated with FS48 (0.1, 1, and 10 μM) and 100 nM MgTx for 30 min before stimulated with PMA/ionomycin (50 ng/ml; 1 μg/ml) for 24 h. The cells treated with PBS were used as a negative control. Then, the supernatants were collected after centrifugation, and the concentration of TNF-α and IL-2 was determined with ELISA kit (Thermo Fisher Scientific Inc) according to the manufacturer's instructions. Each experiment was repeated at least three times.

Western blot analysis

Jurkat T cells were cultured in 6-well plates and incubated with 3 μM FS48 and 100 nM MgTx for indicated time in the presence or absence of PMA/ionomycin, the cells treated with PBS were used as a negative control. The cells were lysed with RIPA buffer and prepared for Western blot analysis as previously reported (48). Primary antibodies against Kv1.3 (4 °C, 16 h, 1: 200), p65, p38, p-p38, ERK, p-ERK, JNK, p-JNK, Histone H3, NF-κB p65, NFATc1, GAPDH, (4 °C, 16 h, 1:1000), and horseradish peroxidase–conjugated secondary antibodies (26 °C, 1 h, 1:2000) were applied, respectively. Chemiluminescence signals were detected and captured with Kodak XAR film. GAPDH and Histone H3 were used as the internal reference for proteins in cytoplasm and cell nucleus, respectively. All experiments were carried out independently at least three times.

Intracellular calcium measurement

Intracellular Ca^{2+} concentration was measured with both flow cytometry and microplate reader assays. For flow cytometry assay, Jurkat T cells were cultured in a 6-well plate at a density of 1×10^6 cells/ml and respectively treated with 3 μM FS48 and 100 nM MgTx for 1 h before incubation with PMA/ionomycin (50 ng/ml; 1 μg/ml) for 6 h, the cells treated with PBS were used as a negative control. The cells were washed with PBS for three times and loaded with 5 μM Fluo4-AM for 45 min. Then, the cells were collected after centrifugation and resuspended with PBS. Intracellular Ca^{2+} concentrations were determined using the FACScan flow cytometer (Becton Dickinson Company) with excitation wavelength 488 nm and emission wavelength 525 nm, and a total of 10,000 events were collected of each sample. FlowJo (ver. 7.6) software was used to analyze the FACScan flow cytometry data. For microplate reader assay, Jurkat T cells were collected and washed with Ca^{2+} free Ringer's solution, which were composed of (in mM): 155 NaCl, 5 HEPES, 4.5 KCl, 3 $MgCl_2$, 10 Glucose, 1 EGTA. The cells were incubated with 2 μM Fluo4-AM in Ca^{2+} free Ringer's solution for 30 min after washed twice, a total of 5×10^4/well cells were seed into a 96-well black plate and treated with FS48 (0.1, 1, 10 μM) for 20 min, the cells treated with PBS were used as a negative control. After incubation, the cells were added with 1 μM TG to elicit Ca^{2+} release in Ca^{2+} free Ringer's solution, and fluorescent signals were read using microplate spectrophotometer (Tecan Company) with excitation wavelength 488 nm and emission wavelength 525 nm at 10 s intervals. At the fifth minute point, a final concentration of 2 mM $CaCl_2$ was add to stimulate Ca^{2+} influx into the cell. The Ca^{2+} influx response was presents as $\Delta F/F_0$ ($\Delta F = F - F_0$, where F_0 is the mean value of the background fluorescence value).

Knockdown of Kv1.3 expression with siRNA

Jurkat T cells were transfected with siRNA to knockdown the expression of Kv1.3 channel as described in our previous study (16). Western blot analysis was carried out to determine the efficiency of siRNA knockdown rate. The most effective siRNA was selected for further experiment. The cells were transfected with most effective siRNA for 24 h and further treated with FS48, MgTx, and PMA/ionomycin as described above, and the supernatants were used to measure the protein levels of TNF-α and IL-2 with ELISA kit according to the manufacturer's instructions.

Table 1
Primers used for qRT-PCR

Name	Forward	Reverse
TNF-α	5′-CACAGTGAAGTGCTGGCAAC-3′	5′-AGGAAGGCCTAAGGTCCACT-3′
IL-2	5′-AGAACTCAAACCTCTGGAGGAAG-3′	5′-GCTGTCTCATCAGCATATTCACA-3′
KCNA3	5′-TGCGGTTCTTCGCTTGTC-3′	5′-GTCCATTGCCCTGTCGTT-3′
GAPDH	5′-GTGAAGGTCGGTGTGAACGGATT-3′	5′-GGAGATGATGACCCTTTTGGCTC-3′

Prevention of active DTH

Eight-week-old female Wistar rats (180–200 g) were purchased from the Laboratory Animal Center of Southern Medical University and housed in plastic cages (relative humidity: 40%–70%; temperature: 20–26 °C) with a 12 h light/dark cycle and supplied with food and water *ad libitum*. The Animal Care and Use Ethics of Southern Medical University approved all protocols and procedures involving live animals in the present study. The rats were randomly divided into control, model, and FS48-treated groups. Model and FS48-treated groups were subcutaneously inoculated with 200 μl ovalbumin (1 mg/ml, OVA and complete Freund's adjuvant 1:1 mixed emulsification, Difco) in scruff of the neck to develop memory T cells *in vivo*. After 7 days, rats in model group and FS48-treated group were subcutaneously injected with saline (0.9% NaCl, 0.5 ml/rat) and 2.5 mg/kg FS48 in scruff of the neck respectively for 1 h and then were challenged again with OVA (20 μl, 1 mg/ml) in auricle. Another ear of each rat was injected with equal volume of saline as a control. The thickness of ear was recorded at 0 and 24 h after the second OVA injection using a spring-loaded micrometer (Mitutoyo), Δear thickness represents the inflammatory reaction and DTH severity. Finally, the ears were sheared after euthanasia and prepared for cytokines measurement with ELISA and HE staining analysis according to the manufacturer's instructions.

Statistical analysis

Data analysis and plotting were performed with IBM SPSS Statistics 20.0 software (SPSS Inc). All results are presented as mean ± SD. The significance of three or more groups was analyzed with one-way ANOVA followed by Bonferroni's test. The unpaired Student's t test was used to determine significance between two experimental groups. Statistical significance was set at $p < 0.05$.

Data availability

All data presented and discussed are contained within the article.

Supporting information—This article contains supporting information.

Author contributions—Q. Z., B. Z., and X. X. conceptualization; Q. Z. data curation; Q. Z., Z. D., and X. X. formal analysis; X. X. funding acquisition; Q. Z., W. L., Z. D., and J. C. investigation; Q. Z., W. L., and J. C. methodology; X. C. and X. X. project administration; X. C. resources; Q. Z., W. L., Z. D., B. Z., and J. W. software; X. C. and X. X. supervision; W. L. validation; J. W., X. C., and X. X. writing—original draft; X. C. and X. X. writing—review and editing.

Funding and additional information—This study was funded in part by the Chinese National Natural Science Foundation (No. 31772476, 31861143050, 31911530077 to X. X. and 82070038 to X. C.).

Conflict of interest—The authors declare that they have no conflicts of interest with the contents of this article.

Abbreviations—The abbreviations used are: DTH, delayed-type hypersensitivity; NFATc1, nuclear factor of activate T cells c1; qRT-PCR, quantitative real-time PCR; T_{EM}, effector memory T cell.

References

1. Cahalan, M. D., and Chandy, K. G. (2009) The functional network of ion channels in T lymphocytes. *Immunol. Rev.* **231**, 59–87
2. Feske, S. (2007) Calcium signalling in lymphocyte activation and disease. *Nat. Rev. Immunol.* **7**, 690–702
3. Desai, R., Peretz, A., Idelson, H., Lazarovici, P., and Attali, B. (2000) Ca^{2+}-activated K^+ channels in human leukemic Jurkat T cells. Molecular cloning, biochemical and functional characterization. *J. Biol. Chem.* **275**, 39954–39963
4. Fu, X. X., Du, L. L., Zhao, N., Dong, Q., Liao, Y. H., and Du, Y. M. (2013) 18beta-Glycyrrhetinic acid potently inhibits Kv1.3 potassium channels and T cell activation in human Jurkat T cells. *J. Ethnopharmacol.* **148**, 647–654
5. Zhao, N., Dong, Q., Fu, X. X., Du, L. L., Cheng, X., Du, Y. M., and Liao, Y. H. (2014) Acacetin blocks kv1.3 channels and inhibits human T cell activation. *Cell. Physiol. Biochem.* **34**, 1359–1372
6. Zhao, N., Dong, Q., Qian, C., Li, S., Wu, Q., Ding, D., Li, J., Wang, B., Guo, K., Xie, J., Cheng, X., Liao, Y., and Du, Y. M. (2015) Lovastatin blocks Kv1.3 channel in human T cells: A new mechanism to explain its immunomodulatory properties. *Sci. Rep.* **5**, 17381
7. Zhao, N., Dong, Q., Du, L. L., Fu, X. X., Du, Y. M., and Liao, Y. H. (2013) Potent suppression of Kv1.3 potassium channel and IL-2 secretion by diphenyl phosphine oxide-1 in human T cells. *PLoS One* **8**, e64629
8. Chandy, K. G., and Norton, R. S. (2017) Peptide blockers of Kv1.3 channels in T cells as therapeutics for autoimmune disease. *Curr. Opin. Chem. Biol.* **38**, 97–107
9. Oliveira, I. S., Ferreira, I. G., Alexandre-Silva, G. M., Cerni, F. A., Cremonez, C. M., Arantes, E. C., Zottich, U., and Pucca, M. B. (2019) Scorpion toxins targeting Kv1.3 channels: Insights into immunosuppression. *J. Venom. Anim. Toxins Incl. Trop. Dis.* **25**, e148118
10. Beeton, C., Wulff, H., Standifer, N. E., Azam, P., Mullen, K. M., Pennington, M. W., Kolski-Andreaco, A., Wei, E., Grino, A., Counts, D. R., Wang, P. H., LeeHealey, C. J., Andrew, B. S., Sankaranarayanan, A., Homerick, D., *et al.* (2006) Kv1.3 channels are a therapeutic target for T cell-mediated autoimmune diseases. *Proc. Natl. Acad. Sci. U. S. A.* **103**, 17414–17419
11. Beeton, C., Wulff, H., Barbaria, J., Clot-Faybesse, O., Pennington, M., Bernard, D., Cahalan, M. D., Chandy, K. G., and Beraud, E. (2001) Selective blockade of T lymphocyte K(+) channels ameliorates experimental autoimmune encephalomyelitis, a model for multiple sclerosis. *Proc. Natl. Acad. Sci. U. S. A.* **98**, 13942–13947
12. Koshy, S., Huq, R., Tanner, M. R., Atik, M. A., Porter, P. C., Khan, F. S., Pennington, M. W., Hanania, N. A., Corry, D. B., and Beeton, C. (2014) Blocking Kv1.3 channels inhibits Th2 lymphocyte function and treats a rat model of asthma. *J. Biol. Chem.* **289**, 12623–12632
13. Matheu, M. P., Beeton, C., Garcia, A., Chi, V., Rangaraju, S., Safrina, O., Monaghan, K., Uemura, M. I., Li, D., Pal, S., de la Maza, L. M., Monuki, E., Flugel, A., Pennington, M. W., Parker, I., *et al.* (2008) Imaging of effector memory T cells during a delayed-type hypersensitivity reaction and suppression by Kv1.3 channel block. *Immunity* **29**, 602–614
14. Pennington, M. W., Beeton, C., Galea, C. A., Smith, B. J., Chi, V., Monaghan, K. P., Garcia, A., Rangaraju, S., Giuffrida, A., Plank, D., Crossley, G., Nugent, D., Khaytin, I., Lefievre, Y., Peshenko, I., *et al.* (2009) Engineering a stable and selective peptide blocker of the Kv1.3 channel in T lymphocytes. *Mol. Pharmacol.* **75**, 762–773
15. Pennington, M. W., Czerwinski, A., and Norton, R. S. (2018) Peptide therapeutics from venom: Current status and potential. *Bioorg. Med. Chem.* **26**, 2738–2758

16. Deng, Z., Zeng, Q., Tang, J., Zhang, B., Chai, J., Andersen, J. F., Chen, X., and Xu, X. (2021) Anti-inflammatory effects of FS48, the first potassium channel inhibitor from the salivary glands of the flea Xenopsylla cheopis. *J. Biol. Chem.* **296**, 100670
17. Leonard, R. J., Garcia, M. L., Slaughter, R. S., and Reuben, J. P. (1992) Selective blockers of voltage-gated K^+ channels depolarize human T lymphocytes: Mechanism of the antiproliferative effect of charybdotoxin. *Proc. Natl. Acad. Sci. U. S. A.* **89**, 10094–10098
18. Vennekamp, J., Wulff, H., Beeton, C., Calabresi, P. A., Grissmer, S., Hansel, W., and Chandy, K. G. (2004) Kv1.3-blocking 5-phenylalkoxypsoralens: A new class of immunomodulators. *Mol. Pharmacol.* **65**, 1364–1374
19. Hanson, D. C., Nguyen, A., Mather, R. J., Rauer, H., Koch, K., Burgess, L. E., Rizzi, J. P., Donovan, C. B., Bruns, M. J., Canniff, P. C., Cunningham, A. C., Verdries, K. A., Mena, E., Kath, J. C., Gutman, G. A., *et al.* (1999) UK-78,282, a novel piperidine compound that potently blocks the Kv1.3 voltage-gated potassium channel and inhibits human T cell activation. *Br. J. Pharmacol.* **126**, 1707–1716
20. Lin, C. S., Boltz, R. C., Blake, J. T., Nguyen, M., Talento, A., Fischer, P. A., Springer, M. S., Sigal, N. H., Slaughter, R. S., Garcia, M. L., and Et, A. (1993) Voltage-gated potassium channels regulate calcium-dependent pathways involved in human T lymphocyte activation. *J. Exp. Med.* **177**, 637–645
21. Hu, L., Pennington, M., Jiang, Q., Whartenby, K. A., and Calabresi, P. A. (2007) Characterization of the functional properties of the voltage-gated potassium channel Kv1.3 in human $CD4^+$ T lymphocytes. *J. Immunol.* **179**, 4563–4570
22. Chi, V., Pennington, M. W., Norton, R. S., Tarcha, E. J., Londono, L. M., Sims-Fahey, B., Upadhyay, S. K., Lakey, J. T., Iadonato, S., Wulff, H., Beeton, C., and Chandy, K. G. (2012) Development of a sea anemone toxin as an immunomodulator for therapy of autoimmune diseases. *Toxicon* **59**, 529–546
23. Li, Z., Liu, W. H., Han, S., Peng, B. W., Yin, J., Wu, Y. L., He, X. H., and Li, W. X. (2012) Selective inhibition of CCR7(-) effector memory T cell activation by a novel peptide targeting Kv1.3 channel in a rat experimental autoimmune encephalomyelitis model. *J. Biol. Chem.* **287**, 29479–29494
24. He, X. H., Zeng, Y. Z., Xu, L. H., Sun, H., Zhen, L., and Fang, D. J. (2002) Influences of protein kinase C inhibitors on the expression of IL-2 and IFN-γ by human T-lymphocytes. *Chin. J. Pathophysiol.* **5**, 522–525
25. Villalonga, N., David, M., Bielanska, J., Gonzalez, T., Parra, D., Soler, C., Comes, N., Valenzuela, C., and Felipe, A. (2010) Immunomodulatory effects of diclofenac in leukocytes through the targeting of Kv1.3 voltage-dependent potassium channels. *Biochem. Pharmacol.* **80**, 858–866
26. Conforti, L., Petrovic, M., Mohammad, D., Lee, S., Ma, Q., Barone, S., and Filipovich, A. H. (2003) Hypoxia regulates expression and activity of Kv1.3 channels in T lymphocytes: A possible role in T cell proliferation. *J. Immunol.* **170**, 695–702
27. Jang, S. H., Byun, J. K., Jeon, W. I., Choi, S. Y., Park, J., Lee, B. H., Yang, J. E., Park, J. B., O'Grady, S. M., Kim, D. Y., Ryu, P. D., Joo, S. W., and Lee, S. Y. (2015) Nuclear localization and functional characteristics of voltage-gated potassium channel Kv1.3. *J. Biol. Chem.* **290**, 12547–12557
28. Attali, B., Romey, G., Honore, E., Schmid-Alliana, A., Mattei, M. G., Lesage, F., Ricard, P., Barhanin, J., and Lazdunski, M. (1992) Cloning, functional expression, and regulation of two K^+ channels in human T lymphocytes. *J. Biol. Chem.* **267**, 8650–8657
29. Proud, C. G. (1994) Translation. Turned on by insulin. *Nature* **371**, 747–748
30. Zhou, Q. L., Wang, T. Y., Li, M., and Shang, Y. X. (2018) Alleviating airway inflammation by inhibiting ERK-NF-kappaB signaling pathway by blocking Kv1.3 channels. *Int. Immunopharmacol.* **63**, 110–118
31. Kan, X. H., Gao, H. Q., Ma, Z. Y., Liu, L., Ling, M. Y., and Wang, Y. Y. (2016) Kv1.3 potassium channel mediates macrophage migration in atherosclerosis by regulating ERK activity. *Arch. Biochem. Biophys.* **591**, 150–156
32. Martinez-Marmol, R., Comes, N., Styrczewska, K., Perez-Verdaguer, M., Vicente, R., Pujadas, L., Soriano, E., Sorkin, A., and Felipe, A. (2016) Unconventional EGF-induced ERK1/2-mediated Kv1.3 endocytosis. *Cell. Mol. Life Sci.* **73**, 1515–1528
33. Ehring, G. R., Kerschbaum, H. H., Eder, C., Neben, A. L., Fanger, C. M., Khoury, R. M., Negulescu, P. A., and Cahalan, M. D. (1998) A nongenomic mechanism for progesterone-mediated immunosuppression: Inhibition of K^+ channels, Ca^{2+} signaling, and gene expression in T lymphocytes. *J. Exp. Med.* **188**, 1593–1602
34. Li, T., Wong, V. K., Yi, X. Q., Wong, Y. F., Zhou, H., and Liu, L. (2009) Pseudolaric acid B suppresses T lymphocyte activation through inhibition of NF-kappaB signaling pathway and p38 phosphorylation. *J. Cell. Biochem.* **108**, 87–95
35. Wei, N., Li, T., Chen, H., Mei, X., Cao, B., and Zhang, Y. Y. (2013) The immunosuppressive activity of pseudolaric acid B on T lymphocytes *in vitro*. *Phytother. Res.* **27**, 980–985
36. Engstrom, L., Pinzon-Ortiz, M. C., Li, Y., Chen, S. C., Kinsley, D., Nelissen, R., Fine, J. S., Mihara, K., and Manfra, D. (2009) Characterization of a murine keyhole limpet hemocyanin (KLH)-delayed-type hypersensitivity (DTH) model: Role for p38 kinase. *Int. Immunopharmacol.* **9**, 1218–1227
37. Li, T., Wang, W., Zhao, J. H., Zhou, X., Li, Y. M., and Chen, H. (2015) Pseudolaric acid B inhibits T-cell mediated immune response *in vivo* via p38MAPK signal cascades and PPARγ activation. *Life Sci.* **121**, 88–96
38. Campbell, J., Ciesielski, C. J., Hunt, A. E., Horwood, N. J., Beech, J. T., Hayes, L. A., Denys, A., Feldmann, M., Brennan, F. M., and Foxwell, B. M. (2004) A novel mechanism for TNF-alpha regulation by p38 MAPK: Involvement of NF-kappa B with implications for therapy in rheumatoid arthritis. *J. Immunol.* **173**, 6928–6937
39. Agrawal, S., Gollapudi, S., Su, H., and Gupta, S. (2011) Leptin activates human B cells to secrete TNF-alpha, IL-6, and IL-10 via JAK2/STAT3 and p38MAPK/ERK1/2 signaling pathway. *J. Clin. Immunol.* **31**, 472–478
40. Li, Q., Yu, H., Zinna, R., Martin, K., Herbert, B., Liu, A., Rossa, C. J., and Kirkwood, K. L. (2011) Silencing mitogen-activated protein kinase-activated protein kinase-2 arrests inflammatory bone loss. *J. Pharmacol. Exp. Ther.* **336**, 633–642
41. Beeton, C., Barbaria, J., Giraud, P., Devaux, J., Benoliel, A. M., Gola, M., Sabatier, J. M., Bernard, D., Crest, M., and Beraud, E. (2001) Selective blocking of voltage-gated K^+ channels improves experimental autoimmune encephalomyelitis and inhibits T cell activation. *J. Immunol.* **166**, 936–944
42. Koo, G. C., Blake, J. T., Talento, A., Nguyen, M., Lin, S., Sirotina, A., Shah, K., Mulvany, K., Hora, D. J., Cunningham, P., Wunderler, D. L., McManus, O. B., Slaughter, R., Bugianesi, R., Felix, J., *et al.* (1997) Blockade of the voltage-gated potassium channel Kv1.3 inhibits immune responses *in vivo*. *J. Immunol.* **158**, 5120–5128
43. Ye, F., Hu, Y., Yu, W., Xie, Z., Hu, J., Cao, Z., Li, W., and Wu, Y. (2016) The scorpion toxin analogue BmKTX-D33H as a potential Kv1.3 channel-selective immunomodulator for autoimmune diseases. *Toxins (Basel)* **8**, 115
44. Wang, Z., Chen, Z., Chen, T., Yi, T., Zheng, Z., Fan, H., and Chen, Z. (2017) Berberine attenuates inflammation associated with delayed-type hypersensitivity via suppressing Th1 response and inhibiting apoptosis. *Inflammation* **40**, 221–231
45. Kobayashi, K., Kaneda, K., and Kasama, T. (2001) Immunopathogenesis of delayed-type hypersensitivity. *Microsc. Res. Tech.* **53**, 241–245
46. Serrano-Albarras, A., Estadella, I., Cirera-Rocosa, S., Navarro-Perez, M., and Felipe, A. (2018) Kv1.3: A multifunctional channel with many pathological implications. *Expert Opin. Ther. Targets* **22**, 101–105
47. Xu, X., Zhang, B., Yang, S., An, S., Ribeiro, J. M., and Andersen, J. F. (2016) Structure and function of FS50, a salivary protein from the flea Xenopsylla cheopis that blocks the sodium channel NaV1.5. *Sci. Rep.* **6**, 36574
48. Deng, Z., Chai, J., Zeng, Q., Zhang, B., Ye, T., Chen, X., and Xu, X. (2019) The anticancer properties and mechanism of action of tablysin-15, the RGD-containing disintegrin, in breast cancer cells. *Int. J. Biol. Macromol.* **129**, 1155–1167